4. C. Topfer, "Comments on the article 'Boundary layers in fluids with low friction' by H. Blasius," Z. Math. Phys., 397-398 (1912).
5. L. Howarth, "On the solution of the laminar boundary-layer equations," Proc. R. Soc., London, A164, 547-579 (1938).
6. H. Schlichting, Boundary Layer Theory, 6th Ed., McGraw-Hill, New York (1968), p. 129.
7. L. Rosenhead (editor), Laminar Boundary Layers, Oxford Univ. Press (1963).
8. S. I. Pai, Viscous-Flow Theory: Laminar Flow, Vol. 1, Van Nostrand, New York (1965).
9. J. G. Oldroyd, "On the formulation of rheological equations of state," Proc. R. Soc., London, 523-541 (1949).
10. K. Walters, "The solution of flow problems in the case of materials with memory, Part. 1," J. Mec., 1, 479-488 (1962).
11. D. W. Beard and K. Walters, "Elastic-viscous boundary-layer flow, Part 1: Two-dimensional flow near a stagnation point," Proc. Cambridge Phil. Soc., 60, 667-674 (1964).
12. V. M. Soundalgekar and N. V. Vighnesam (in press).

ISOTHERMAL FLOW OF A NON-NEWTONIAN FLUID THROUGH THE CHANNEL OF A VOLUTE-TYPE DISK PUMP UNDER CONDITIONS OF COMPLEX SHEAR

V. I. Yankov and V. A. Makarov

UDC 532.542:532.135

A study is made pertaining to steady laminar flow of an anomalously viscous fluid between two rigid disks in one of which the thread has been cut in the form of an Archimedes spiral.

The advantages of a volute-type disk pump with the thread cut in the form of an Archimedes spiral over a conventional volute-type pump are the simplicity of its construction, the possibility of regulating the clearances between the spiral ridges and the smooth other disk, and the higher pressure head developed. The use of such pumps in industry is not widespread owing to, apparently, not only the large axial forces developing in them (which, by the way, can be successfully reduced by adoption of the bilateral volute construction) but also the unavailability of a design method.

We will consider the isothermal flow of a non-Newtonian fluid through a volute-type disk pump consisting of two parallel rigid disks in one of which the thread has been cut in the form of an Archimedes spiral (Fig. 1a). The threaded disk is stationary, while the smooth disk rotates at a constant angular velocity ω_0. It will be assumed in the formulation of the problem that the channel width S is much larger than the channel depth H and that there are no clearances between the spiral ridges and the smooth disk, the flow of the fluid being steady and laminar. All calculations will refer to the median line of the spiral (dash–dot line on the diagram), considering that the tangential velocity of the smooth disk $V_0 = r\omega_0$ as well as the lead angle of the spiral δ and the pressure gradients $\partial p/\partial \varphi = A_\varphi$, $\partial p/\partial r = A_r$ vary only along the channel (in the φ direction) while remaining constant across its width. Let the inside radius and the outside radius of the Archimedes spiral be r_i and r_o, respectively. The velocity component in the z direction will be disregarded.

In solving this problem we are mostly concerned about the pressure gradients $\partial p/\partial x = A_x$, $\partial p/\partial y = A_y$ and the flow rate Q_x. Accordingly, the vector representing the tangential velocity of the smooth disk V_0 can be resolved into two components: $V_x = V_0 \cos \delta$ and $V_y = V_0 \sin \delta$ (Fig. 1b).

The equations of motion, in projection on the axes φ and r, can be written as

$$\frac{\partial \tau_{\varphi z}}{\partial z} = \frac{A_\varphi}{r}, \quad \frac{\partial \tau_{rz}}{\partial z} = A_r - \rho \frac{V_\varphi^2}{r}. \tag{1}$$

An analysis of the solution to Eqs. (1) for a Newtonian fluid has revealed that, with

All-Union Scientific-Research Institute of Synthetic Fibers, Kalinin. Translated from Inzhenerno-Fizicheskii Zhurnal, Vol. 40, No. 2, pp. 231-237, February, 1981. Original article submitted February 4, 1980.

0022-0841/81/4002-0133$07.50

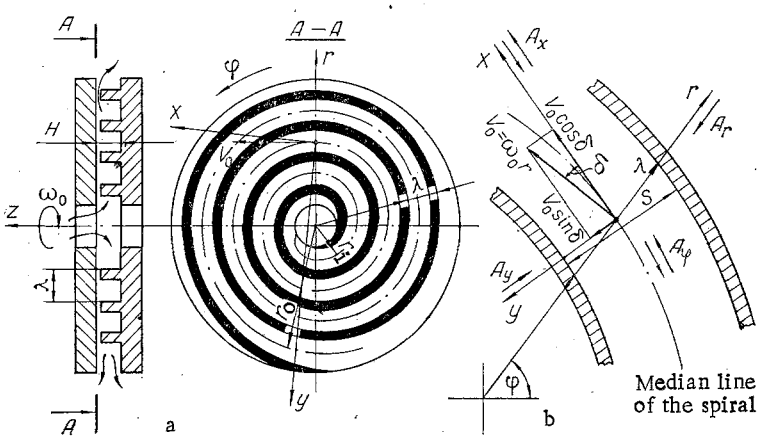

Fig. 1. Volute-type disk pump (a) and its schematic design diagram (b).

$N_{Re} \leq 10$, addition of the term $\rho V_\varphi^2/r$ to the equation of motion in the r-projection has almost no effect on the velocity profiles and on the Δp (pressure head)–Q_x (flow rate) characteristics of a volute-type disk pump. Considering that such pumps are intended for transfer of high-viscosity fluids and rarely operate even with $N_{Re} = 1$, we disregard the centrifugal term in Eqs. (1) so that the solution can be written as

$$\tau_{\varphi z} = \frac{A_\varphi}{r}(z - Hc_1),\ \tau_{rz} = A_r(z - Hc_2). \tag{2}$$

As the rheological equation for such a fluid, we will use a power law, viz., in this case

$$\bar{\tau} = B\left[\left(\frac{\partial V_\varphi}{\partial z}\right)^2 + \left(\frac{\partial V_r}{\partial z}\right)^2\right]^{\frac{n-1}{2}}\bar{\Delta}. \tag{3}$$

For the solution of the problem we will use the following dimensionless variables and parameters:

$$\xi = \frac{z}{H},\ a = \frac{A_y}{|A_x|},\ \frac{V_\varphi}{\omega_0 r} = V_1,\ \frac{V_r}{\omega_0 r} = V_2,\ \frac{V_x}{\omega_0 r} = V_3,\ \frac{V_y}{\omega_0 r} = V_4,\ \alpha = \frac{\omega_0 r}{H}\left[\frac{B}{H|A_x|\cos\delta}\right]^{\frac{1}{n}}. \tag{4}$$

In the dimensionless quantities (4), we then write the boundary conditions of the problem as

$$V_1 = V_2 = 0 \text{ at } \xi = 0;\ V_1 = 1,\ V_2 = 0 \text{ at } \xi = 1. \tag{5}$$

Inasmuch as we will subsequently be interested in the projections of the fluid velocities on axes x and y, pressure gradients A_φ and A_r can be expressed through their components A_X and A_Y as follows:

$$A_\varphi = (A_x\cos\delta + A_y\sin\delta)\,r,\ A_r = A_x\sin\delta - A_y\cos\delta. \tag{6}$$

A simultaneous solution of Eqs. (2) and (3), using the dimensionless quantities (4) and the expressions (6), yields [1]

$$\frac{\partial V_1}{\partial\xi} = \frac{1}{\pm\alpha F}(1 + a\,\mathrm{tg}\,\delta)(\xi - c_1),\ \frac{\partial V_2}{\partial\xi} = \frac{1}{\pm\alpha F}(\mathrm{tg}\,\delta - a)(\xi - c_2),^* \tag{7}$$

where

$$F = [(1 + a\,\mathrm{tg}\,\delta)^2(\xi - c_1)^2 + (\mathrm{tg}\,\delta - a)^2(\xi - c_2)^2]^{\frac{n-1}{2n}}.$$

*The signs plus and minus before α correspond to flow of the fluid with $A_X \geq 0$ and $A_X < 0$, respectively. The corresponding sign before a will be determined automatically in the course of the solution of the problem.

Integration of expressions (7), using the first pair of boundary conditions (5), yields for the fluid velocities in the directions of axes φ and r

$$V_1 = \frac{1 + a\,\mathrm{tg}\,\delta}{\pm\alpha} \int_0^{\xi} \frac{(\xi - c_1)}{F}\, d\xi,\quad V_2 = \frac{\mathrm{tg}\,\delta - a}{\pm\alpha} \int_0^{\xi} \frac{(\xi - c_2)}{F}\, d\xi, \tag{8}$$

respectively. Considering that $V_3 = V_1 \cos\delta + V_2 \sin\delta$ and $V_4 = V_1 \sin\delta - V_2 \cos\delta$, we finally obtain for the dimensionless velocities V_3 and V_4 in the directions of axes x and y, respectively,

$$\begin{aligned} V_3 &= \frac{1 + a\,\mathrm{tg}\,\delta}{\pm\alpha} \cos\delta \int_0^{\xi} \frac{(\xi - c_1)}{F}\, d\xi + \frac{\mathrm{tg}\,\delta - a}{\pm\alpha} \sin\delta \int_0^{\xi} \frac{(\xi - c_2)}{F}\, d\xi, \\ V_4 &= \frac{1 + a\,\mathrm{tg}\,\delta}{\pm\alpha} \sin\delta \int_0^{\xi} \frac{(\xi - c_1)}{F}\, d\xi - \frac{\mathrm{tg}\,\delta - a}{\pm\alpha} \cos\delta \int_0^{\xi} \frac{(\xi - c_2)}{F}\, d\xi. \end{aligned} \tag{9}$$

The flow rates, per unit channel width and per unit channel length, in the directions of axes x and y are then

$$q_x = \frac{Q_x}{\omega_0 r H S} = \int_0^1 V_3 d\xi,\quad q_y = \frac{Q_y}{\omega_0 r H l} = \int_0^1 V_4 d\xi. \tag{10}$$

Inserting expressions (9) into expressions (10) and integrating by parts yields

$$\begin{aligned} q_x &= \frac{1 + a\,\mathrm{tg}\,\delta}{\pm\alpha} \cos\delta \int_0^1 \frac{(\xi - c_1)(1 - \xi)}{F}\, d\xi + \frac{\mathrm{tg}\,\delta - a}{\pm\alpha} \sin\delta \int_0^1 \frac{(\xi - c_2)(1 - \xi)}{F}\, d\xi, \\ q_y &= \frac{1 + a\,\mathrm{tg}\,\delta}{\pm\alpha} \sin\delta \int_0^1 \frac{(\xi - c_1)(1 - \xi)}{F}\, d\xi - \frac{\mathrm{tg}\,\delta - a}{\pm\alpha} \cos\delta \int_0^1 \frac{(\xi - c_2)(1 - \xi)}{F}\, d\xi. \end{aligned} \tag{11}$$

In order to solve the problem, therefore, it is necessary to know the integration constants c_1 and c_2 as well as parameter a and the magnitude of α (or of pressure gradient A_X). For finding these quantities, we use the second pair of boundary conditions (5) and constraints which must be imposed on the flow rates in the directions x and y ($q_y = 0$, and q_x is given in the problem), with which we obtain a system of four transcendental equations

$$\begin{aligned} &\frac{1 + a\,\mathrm{tg}\,\delta}{\pm\alpha} \int_0^1 \frac{(\xi - c_1)}{F}\, d\xi - 1 = 0, \\ &\int_0^1 \frac{(\xi - c_2)}{F}\, d\xi = 0, \\ &\frac{1 + a\,\mathrm{tg}\,\delta}{\pm\alpha} \sin\delta \int_0^1 \frac{(\xi - c_1)(1 - \xi)}{F}\, d\xi - \frac{\mathrm{tg}\,\delta - a}{\pm\alpha} \cos\delta \int_0^1 \frac{(\xi - c_2)(1 - \xi)}{F}\, d\xi = 0, \\ &\frac{1 + a\,\mathrm{tg}\,\delta}{\pm\alpha} \cos\delta \int_0^1 \frac{(\xi - c_1)(1 - \xi)}{F}\, d\xi + \frac{\mathrm{tg}\,\delta - a}{\pm\alpha} \sin\delta \int_0^1 \frac{(\xi - c_2)(1 - \xi)}{F}\, d\xi - q_x = 0. \end{aligned} \tag{12}$$

While solving the problem, one must bear in mind that the lead angle δ of an Archimedes spiral is not a constant quantity but a function of the angular coordinate φ, i.e.,

$$\delta = 90° - \mathrm{arctg}\,\frac{1}{\varphi},$$

or, since for an Archimedes spiral

$$r = \frac{\lambda}{2\pi}\varphi, \tag{13}$$

a function of the radius

$$\delta = 90° - \operatorname{arctg}\frac{\lambda}{2\pi r}. \tag{14}$$

The length of an Archimedes spiral is

$$l = \frac{\lambda}{4\pi}(\varphi_o^2 - \varphi_i^2) = \frac{\pi}{\lambda}(r_o^2 - r_i^2). \tag{15}$$

The pressure head developed by a volute-type disk pump is

$$\Delta p = \int_0^l A_x dx. \tag{16}$$

Inasmuch as the solution to the system of equations (12) yields the value of α, inserting into expression (16) the value of A_X in terms of α according to relation (4) will, with relations (13) and (15) taken into account, yields

$$\Delta p = \frac{2\pi B}{\lambda H}\left(\frac{\omega_0}{H}\right)^n \int_{r_i}^{r_o}\left[\pm\left(\frac{r}{\alpha}\right)^n\right]\frac{r dr}{\cos\delta} = \frac{\lambda B}{2\pi H}\left(\frac{\lambda\omega_0}{2\pi H}\right)^n \int_{\varphi_i}^{\varphi_o}\left[\pm\left(\frac{\varphi}{\alpha}\right)^n\right]\frac{\varphi d\varphi}{\cos\delta}. \tag{17}$$

The power drawn by a volute-type disk pump can be calculated as

$$dN = (\tau_{xz}|_{z=H}\cos\delta + \tau_{yz}|_{z=H}\sin\delta)\,\omega_0 r S dx = \tau_{\varphi z}|_{z=H}\,\omega_0 r S dx. \tag{18}$$

Integrating this expression (18), after the value of the shearing stress $\tau_{\varphi z}$ according to relation (2) has been inserted into it, yields

$$N = H\omega_0\int_0^l A_x(1 + a\operatorname{tg}\delta)(1 - c_1)\,Sr\cos\delta\,dx = \frac{2\pi B}{\lambda}\left(\frac{\omega_0}{H}\right)^n\omega_0\times$$

$$\times\int_{r_i}^{r_o}\left[\pm\left(\frac{r}{\alpha}\right)^n\right](1 + a\operatorname{tg}\delta)(1 - c_1)\,Sr^2 dr = \left(\frac{\lambda}{2\pi}\right)^{n+2}\left(\frac{\omega_0}{H}\right)^n\omega_0 B\int_{\varphi_i}^{\varphi_o}\left[\pm\left(\frac{\varphi}{\alpha}\right)^n\right](1 + a\operatorname{tg}\delta)(1 - c_1)\,S\varphi^2 d\varphi. \tag{19}$$

An analysis to the solution to our problem reveals that pressure gradient A_X varies along the spiral not only in magnitude but also in direction. At some flow rate $q_X = q_{Xo}$ in the channel where $r = r_o$ there can be found a channel section where $A_X = 0$. Therefore, $A_X \leqslant 0$ and is directed toward the center of the spiral along the channel segment $r_o \leqslant r \leqslant r_o$ but $A_X \geqslant 0$ and is directed outward along the channel segment $r_i \leqslant r \leqslant r_o$. Depending on the magnitude of q_X, the section with a zero pressure gradient can fall beyond the channel and then $A_X > 0$ along the entire channel $r_i \leqslant r \leqslant r_o$.

For specific calculations we have selected the following values of parameters: r_i = 0.06 m, r_o = 0.125 m, H = 0.01 m, S = 0.022 m, λ = 0.025 m, ω_o = 10 sec^{-1}; B = 205 $N\cdot sec^{0.4}\cdot m^{-2}$, n = 0.4, and p_i = 0.

The system of equations (12) was solved numerically with the aid of a computer. The results of calculations are shown in Figs. 2 and 3.

The graph in Fig. 2a depicts the distribution of the pressure gradient A_X along the channel at various flow rates $Q_X = \omega_o r H S q_X$. This graph indicates that the pressure gradient is always positive when $Q_X = 0$ (curve 1), but is first negative and then positive when $Q_X = Q_{X,max}$ (curve 5). The points at which these curves cross the axis of abscissas correspond to sections where $A_X = 0$. Curves 2-4 have been plotted for intermediate values of the flow rate. The graph indicates also that, as the flow rate is increased, the section at which $A_X = 0$ shifts away from the inlet toward the outlet, and at flow rates higher than $Q_{X,max}$ (curves 6, 7) it can pass beyond the channel. It is noteworthy, furthermore, that the pressure gradient A_X at any flow rate always increases with the radius, because the tangential velocity of the smooth disk increases with the radius.

The graph in Fig. 2b depicts the distribution of the pressure head along the spiral

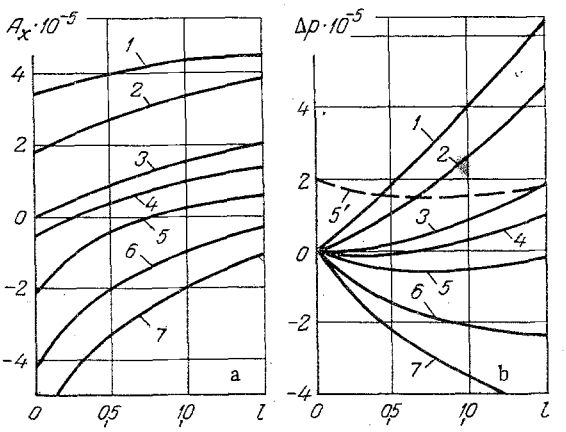

Fig. 2. Distribution of the pressure gradient A_x, N/m^3 (a) and of the pressure head Δp, N/m^2 (b) along the channel at various flow rates Q_x, m^3/sec: 1) 0; 2) $3 \cdot 10^{-5}$ m^3/sec; 3) $6.6 \cdot 10^{-5}$ m^3/sec; 4) $8.03 \cdot 10^{-5}$ m^3/sec; 5) $10.58 \cdot 10^{-5}$ m^3/sec; 6) $15.2 \cdot 10^{-5}$ m^3/sec; 7) $18 \cdot 10^{-5}$ m^3/sec. l in m.

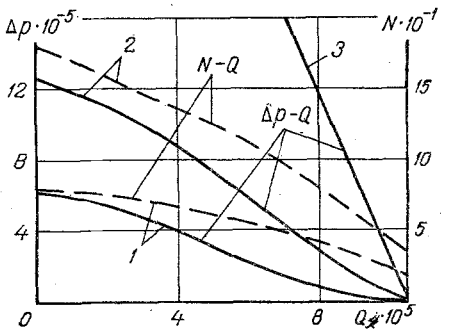

Fig. 3. Dependence of the pressure head Δp (N/m^2) and of the input power N ($N \cdot m/sec$) on the flow rate Q (m^3/sec) and on the viscous anomaly: 1) n = 0.4 and B = 205 $N \cdot sec^{0.4} \cdot m^{-2}$; 2) n = 0.6 and B = 137 $N \cdot sec^{0.6} \cdot m^{-2}$; 3) n = 1.0 and B = 62.5 $N \cdot sec \cdot m^{-2}$.

channel. At a zero flow rate (curve 1) or at a low flow rate (curve 2) the pressure of the fluid rises continuously along the channel, while at high flow rates (curve 5) it first drops and then rises. It is important to note that at flow rates close to $Q_{x,max}$ or higher than that (curves 5-7) the entire pressure curve lies within the negative range. The theoretical minimum pressure head can reach very low levels, far below minus unity. Since physically this is impossible, such a characteristic cannot be realized in practice. By producing a certain pressure at the pump inlet, however, one can shift the $\Delta p(l)$ curve into the positive range (dash line) and thus realize this characteristic in practice.

The graph in Fig. 3 depicts the dependence of Δp and N on the flow rate Q_x. Curves 1 and curves 2 correspond to the flow of fluids with a viscous anomaly n = 0.4 and n = 0.6 respectively, while curve 3 corresponds to a Newtonian fluid with n = 1. As was to be expected, the pressure head and the power input decrease with decreasing anomaly and this decrease occurs faster, moreover, the farther the fluids depart from a Newtonian one. It must also be noted that the flow rates of fluids with different viscous anomalies are not equal at a $\Delta p = 0$ pressure head and that this difference between their flow rates increases with the lead angle δ (the pitch λ) of the spiral. In our specific example the pitch of the spiral was small, so was the lead angle, consequently the flow rate $Q_{x,max}$ remained almost constant and independent of n.

NOTATION

φ, r, z, cylindrical coordinates; x, y, z, Cartesian coordinates; H and S, channel depth and width; δ, lead angle of the spiral; ω_0, angular velocity of the smooth disk; r_i, r, r_0, inside radius, the radius at any given point, and the outside radius of the spiral along its median line; $A\varphi$, A_r, A_x, A_y, pressure gradients; ρ, density of the fluid; c_1 and c_2, integration constants; $\tau\varphi z$, τrz, τxz, τyz, components of the stress tensor; $V\varphi$, V_r, V_x, V_y, projections of the velocity of the fluid on the axes φ, r, x, y, respectively; τ, stress deviator; B and n, rheological parameters; Δ, strain rate tensor; V_1, V_2, V_3, V_4, dimensionless velocities of the fluid; a, ratio of pressure gradients; Q_x and Q_y, true flow rates in the directions x and y, respectively; $Q_{x,max}$, true flow rate corresponding to a zero pressure head; q_x and q_y, dimensionless flow rates; l and λ, spiral length and pitch; φ_i and φ_0, angular coordinates of the inside endpoint and the outside endpoint of the spiral on its median line; p, pressure; p_i, fluid pressure at the pump inlet; and N, input power.

LITERATURE CITED

1. S. A. Bostandzhiyan, V. I. Boyarchenko, and G. N. Kargopolova, "Flow of a non-Newtonian fluid through the channel of an extruder screw under conditions of complex shear," in: Rheophysics and Rheodynamics of Flow Systems [in Russian], Nauka i Tekhnika, Minsk (1970), pp. 111-121.

AN ARTERIAL HEAT PIPE WITH A GROOVED EVAPORATOR

V. S. Tarasov

UDC 621.565.94

A method is developed for calculating the hydrodynamic heat-transfer boundary of arterial heat pipes with capillary channels having a triangular profile in the evaporator. Comparison with experimental data demonstrates the satisfactory accuracy of the method.

Evaporators for arterial heat pipes (AHP), equipped with ring-shaped capillary channels, e.g., grooves with a triangular profile (V-channels) (Fig. 1), can operate with very dense heat fluxes with high heat-exchange coefficients [1-4]. However, there is no satisfactory theory for calculating the limiting characteristics of such AHP. The difficulty with the hydrodynamic theory developed in [1, 2] is that it does not relate the magnitude of the hydrodynamic heat-transfer boundary (HHTB), which determines the maximum attainable heat flux density in the evaporator, to the pressure losses in the heat carrier in the rest of the AHP and it does not provide a physically correct estimate of the influence of the contact angle on the HHTB.

When heat is input uniformly, all evaporator channels are loaded identically and the HHTB will be determined by the channel in the beginning section of which, for x = 0, the meniscus is curved more strongly than in the neighboring channels [5]. In most cases, this is the edgemost channel that is farthest away from the condensor. For this channel, the following relation is valid:

$$\Delta p_{cap} = \Delta p'_e + \Delta p_{rem} \quad (1)$$

The pressure differential Δp_{rem} in the rest of the AHP causes the meniscus to be curved in the starting section with a radius

$$R_0 = \sigma/\Delta p_{rem}. \quad (2)$$

From the starting section to the end section $x = x_m$, the liquid moves under the action of a capillary pressure gradient, compensating for frictional resistance [1, 2]:

$$\frac{dp'}{dx} = -\frac{dp_{cap}}{dx}. \quad (3)$$

Translated from Inzhenerno-Fizicheskii Zhurnal, Vol. 40, No. 2, pp. 238-243, February, 1981. Original article submitted November 6, 1979.

 0022-0841/81/4002-0138$07.50